Direct Fluorination of the Polyimide Matrimid® 5218: The Formation Kinetics and Physicochemical Properties of the Fluorinated Layers

A. P. Kharitonov,[1] Yu. L. Moskvin,[1] D. A. Syrtsova,[2] V. M. Starov,[3] V. V. Teplyakov[2]

[1]*Institute of Energy Problems of Chemical Physics (Branch), Russian Academy of Sciences, Chernogolovka, 142432, Moscow Region, Russia*
[2]*A. V. Topchiev Institute of Petrochemical Synthesis, Russian Academy of Sciences, Leninskii Prospect, 29, 119991, Moscow, Russia*
[3]*Loughborough University, LE11 3TU, Loughborough, United Kingdom*

Received 7 March 2003; accepted 26 August 2003

ABSTRACT: Fluorinated polymers have a set of unique properties, including improved chemical stability and thermal stability and good barrier and membrane parameters, which are mainly defined by their surface properties. This article presents systematic data on the direct fluorination of the polyimide Matrimid® 5218, a commercially available polymer suitable for the formation of gas-separation hollow fibers. Changing the fluorination conditions (i.e., the fluorinated mixture composition, fluorine partial pressure, and treatment duration) allows the rate of formation of the surface-fluorinated layer over the 0.1–10 μm range to be kept under control. The physicochemical properties of modified layers (i.e., the chemical composition, formation of radicals, refractive index, IR and UV spectra, density, and surface energy) are examined. The thickness of the fluorinated layer (δ_F) depends on the fluorination duration (t): $\delta_F \sim t^{0.5}$. During fluorination, hydrogen atoms are replaced with fluorine, double bonds are saturated with fluorine, and at least one CN bond in the five-member ring is disrupted. Fluorination results in a significant increase in the polymer density, transparency in the visible and ultraviolet regions of spectra, and a reduction of the refractive index. A high concentration of long-living radicals (up to $\sim 5 \times 10^{19}$ radicals/cm^3 of the fluorinated layer) is generated under fluorination. This can be used for subsequent grafting (e.g., with acrylonitrile). © 2004 Wiley Periodicals, Inc. J Appl Polym Sci 92: 6–17, 2004

Key words: polyimides; modification; nanolayers; infrared spectroscopy

INTRODUCTION

Fluorinated polymers are known to have a set of unique properties, including enhanced chemical stability and thermostability and good barrier and membrane properties.[1–6] However, the practical applications of fluoropolymers are restricted because of their high cost and the complexity of their synthesis. Quite often, the application properties of polymer goods are defined mainly by their surface properties. Therefore, it is not necessary to fabricate articles from fluoropolymers. It is simpler, cheaper, and more convenient to apply surface treatments to articles made from commonly used polymers. Plasma[7] or gas-phase[8] fluorination can be used for this. Direct fluorination (i.e., treatment with elemental gaseous fluorine and its gaseous mixtures) can be used to modify the surface properties of polymer articles of any shape. The thickness of a fluorinated layer (δ_F) can be well kept under control over the 0.1–10 μm range. The bulk properties of polymer articles remain unchanged. Because of the high exothermicity of the main elementary stages, fluorination proceeds at room temperature and even at the temperature of liquid nitrogen,[8,9] and it does not need initiation, heating, or catalysts. Direct fluorination is a dry technology because the starting reagents and point end products are gases and solids only. There are well-developed, safe, and reliable ways of neutralizing nonconsumed F_2 and the point end product HF. All of these have led to wide applications for improving the various properties of polymer articles: barrier properties, gas-separation properties of polymer membranes, adhesion, printability, chemical resistance, and so forth. There are some well-developed modifications of the fluorination process: under static conditions and in flow reactors (for previously fabricated polymer articles) and in the course of their fabrication (e.g., during blow molding).[3]

For the majority of the polymers studied by us [e.g., polystyrene, poly(ethylene terephthalate), poly(vinyltrimethylsilane) and its block copolymers, poly(4-methyl-pentene-1), poly(2,6-dimethyl-1,4-phenylene

Correspondence to: A. P. Kharitonov (kharitonbinep.ac.ru).
Contract grant sponsor: Royal Society (United Kingdom).
Contract grant sponsor: Netherlands Organization for Scientific Research; contract grant number: 047.007.006.

© 2004 Wiley Periodicals, Inc.

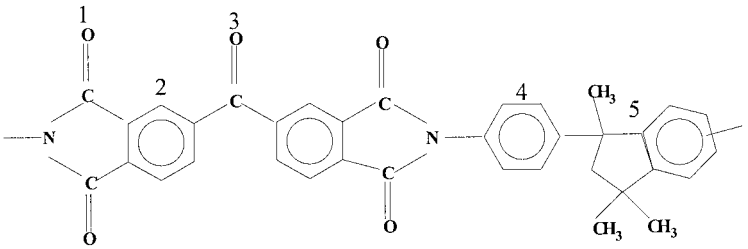

Figure 1 Chemical structure of PI Matrimid® 5218.

oxide), poly(carbonate siloxane) copolymers, polysulfone–polybutadiene block copolymers, and low-density and high-density polyethylenes], the following characteristics of the fluorination process and fluorine-treated polymers have already been studied:[6,8–21]

- The chemical composition, density, and refractive indices of fluorinated polymeric layers.
- The dependence of the rate of formation of fluorinated layers on the treatment duration, fluorine partial pressure, and composition of fluorine-containing mixtures.
- The evaluation of the thickness of the reaction zone between fluorinated and virgin (untreated) polymer layers.
- The termination duration of both long-living radicals and short-living intermediate radicals.
- The influence of the treatment conditions on the permeability, diffusivity, and separation properties for a set of gaseous mixtures.
- The influence of the treatment conditions on the electrochemical stability of polymers.

This article presents systematic data on the fluorination of the polyimide (PI) Matrimid® 5218, a commercially available polymer suitable for the formation of gas-separation hollow fibers.[22]

EXPERIMENTAL

Materials and samples

PI Matrimid® 5218 was supplied by Ciba–Geigy (Switzerland). Its chemical structure is shown in Figure 1.[21] Two types of samples were used: free films (5–50 μm thick) and films (2–10 μm thick) cast from chloroform solutions onto a zinc selenide (ZnSe) support. ZnSe is stable to fluorine and is transparent over a range of 20,000–500 cm^{-1}. Fluorination was performed in closed vessels (300–1000 cm^3). The fluorine that was used had less than 0.1% impurities (mainly oxygen).

Treatment procedure

A polymer sample was inserted into the closed vessel and evacuated to approximately 2–3 $\times$ 10^{-2} Torr for 0.5–1 h for the removal of oxygen and water vapor. Then, the closed vessel (reactor) was filled with a fluorine-containing mixture, and the sample was treated during the necessary time interval. After the treatment, the reactor was evacuated.

Testing equipment and procedure

A Fourier transform infrared spectrometer (FT-02, Lumex, St. Petersburg, Russia) was used to measure the IR spectra. A reaction vessel, equipped with ZnSe windows, was designed to measure the IR spectra during the fluorination or *in vacuo* (the sample was not subjected to atmospheric moisture action). In this case, the treatment was carried out with a fluorine–helium mixture (F_2/He = 1:4, total pressure = 1 bar). The refractive indices were measured with a refractometer (RF-454B, Lomo, Leningrad, Russia). To measure the dependence of δ_F on the treatment duration *in situ* (i.e., the treatment procedure was not interrupted for a single measurement to be carried out), we used the original kinetic interference method with visible light. Flat films with good reflectance (shining surface) were used in these experiments. The kinetics of the change in the intensity of monochromatic light (a helium–neon laser was used as a light source) reflected from the surface of a film was monitored over the course of the fluorination process. Details for kinetic interference spectroscopy can be found in refs. 10, 13–17, and 23.

To measure the surface energy, we used the method proposed in refs. 24 and 25. The spectra in the visible and UV spectral ranges were measured with a Specord ultraviolet–visible spectrometer (Karl Zeiss Jena, Jena, Germany). The concentration of radicals was measured with an EPR-21 electron spin resonance (ESR) spectrometer (Moscow, Russia). The methodology for measuring the density of the thin fluorinated layers is described later.

RESULTS AND DISCUSSION

The transmission visible spectrum of a treated PI film deposited onto a solid support is shown in Figure 2. The spectrum has remarkable interference features

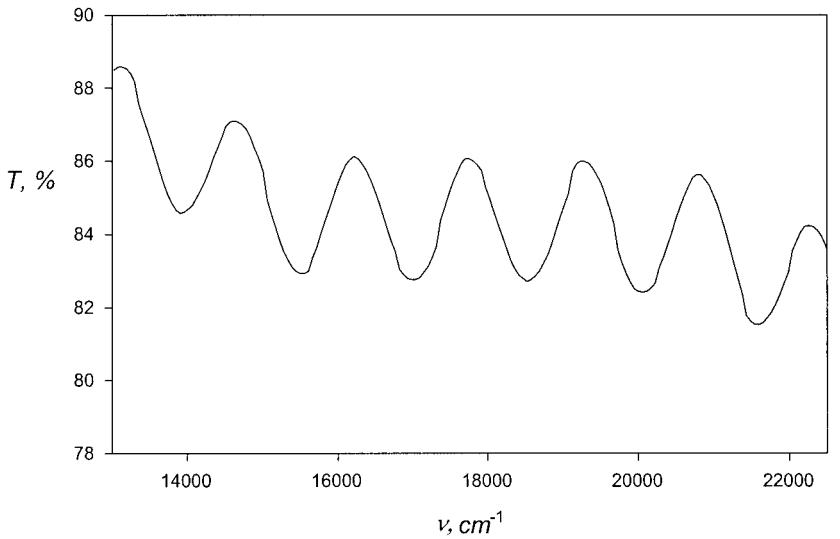

Figure 2 Transmittance (T) of a fluorine-treated PI film (cast and treated on a sapphire substrate) versus ν (δ_F = 2.33 μm). The film was not fluorinated throughout its entire thickness.

due to the double-layer structure of the fluorine-treated film.[9,13–17] It means that a treated film consists of two layers: fluorinated and virgin. Between them, there is a very thin transition (boundary) layer, at which the main chemical transformations take place (Fig. 3). In this case, the rate of formation of a fluorinated layer is limited by the F_2 permeability ($\bar{P}$) through the fluorinated layer to the transition zone. The balance between F_2 consumed in the reaction zone and the amount of F_2 passed through the fluorinated layer can be expressed as follows:

$$B(d\delta_F/dt) = D(dc_F/dx) \quad (1)$$

where D is the diffusion coefficient of fluorine for the fluorinated polymer and c_F is the concentration of fluorine in the fluorinated polymer. The experimentally measured coefficient B is the amount of F_2 [cm^3 (STP)] necessary to form 1 cm^3 of the fluorinated polymer divided by 1 cm^3 of the fluorinated polymer. Assuming that $\delta_b \ll \delta_F$ (where δ_b is a thickness of transition layer) and $c_F(x = \delta_F) \ll c_F(x = 0)$ and that the properties of the fluorinated layer are not changed along the x axis, we have

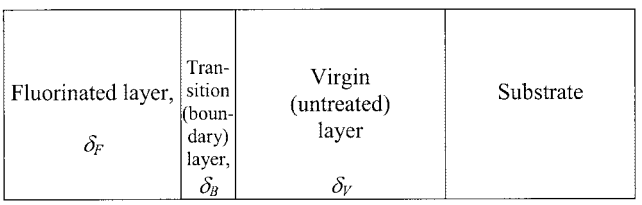

Figure 3 Schematic cross section of a fluorine-treated polymer film cast onto a substrate. The film was not fluorinated throughout its entire thickness.

$$B(d\delta_F/dt) = D[c_F(0)/\delta_F] = DS(p_F/\delta_F) = \bar{P}(p_F/\delta_F) \quad (2)$$

where S is the solubility coefficient of fluorine in a fluorinated polymer [$c_F(x = 0) = Sp_F$ and $\bar{P} = DS$] and p_F is the fluorine partial pressure. Under steady-state fluorination conditions and if p_F and $\bar{P}$ are not changed during fluorination

$$\delta_F = (2/B)(\bar{P}p_F t)^{0.5} = At^{0.5} \quad (3)$$

where A is a coefficient.

To calculate the thickness of a fluorinated polymer layer, we must know the refractive index of the fluorinated polymer (n_F) at the wavelength of the monochromatic light used. For the PI studied, it was measured experimentally: n_F = 1.41 at a wavelength of λ = 632.8 nm (helium–neon laser).

The main experimental results for the kinetics of the formation of a fluorinated layer are shown in Figures 4–8. A treatment was carried out at 22°C (295 K) with undiluted fluorine, a 10:90 F_2/N_2 mixture, and F_2/He mixture (c_F was varied from 2 to 100 vol %), and an F_2/O_2 mixture (the oxygen concentration was varied from 2 to 40 vol %).

Treatment with undiluted fluorine

The dependence of δ_F on the fluorination duration (t) for different p_F values is shown in Figure 4; the dependence of A [see eq. (3)] on p_F is shown in Figure 5. From Figures 4 and 5, we have

$$\delta_F = 4.9 \times 10^{-3} \times p_F^{0.41} \times t^{0.5} \quad (4)$$

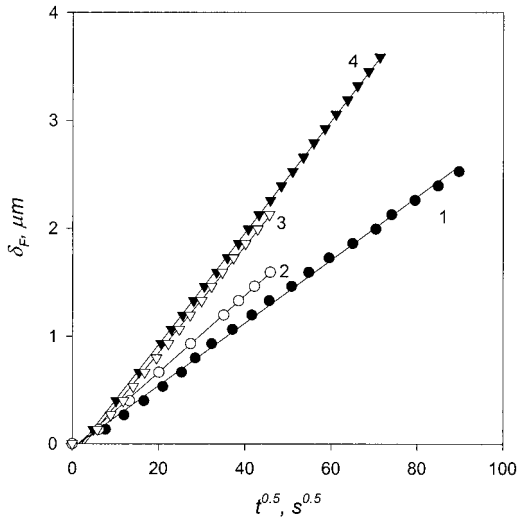

Figure 4 Dependence of δ_F on the square root of t. The undiluted p_F values were (1) 73.5, (2) 147, (3) 294, and (4) 294 Torr; the temperature was 295 K.

Treatment with the F_2/He mixtures

To prevent polymeric articles from being damaged, usually diluted mixtures at atmospheric pressure and room temperature are used in industry. The dependence of δ_F on t for F_2/He mixtures of various compositions but at the same p_F values is shown in Figure 6. The addition of helium to fluorine practically does not influence the rate of formation of a fluorinated layer when p_F is kept at the steady-state level (Fig. 6).

Treatment with the F_2/N_2 mixtures

δ_F (μm) depends on t (s) as a square root:

$$\delta_F = 1.45 \times 10^{-3} \times {p_F}^{0.74} \times t^{0.5} \qquad (5)$$

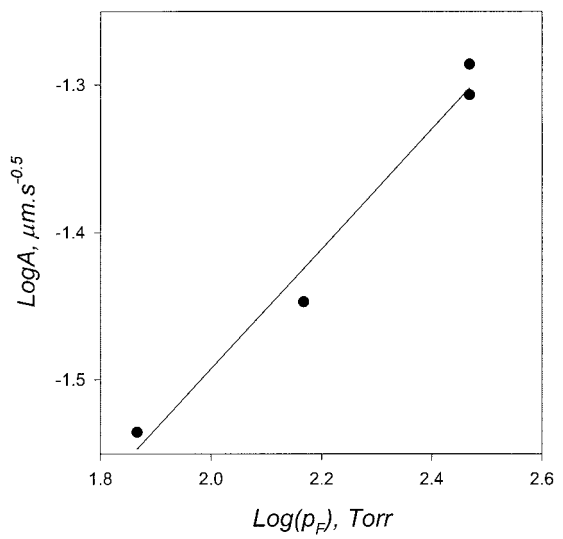

Figure 5 Dependence of A [see eq. (3)] on p_F for curves 1–4 in Figure 4.

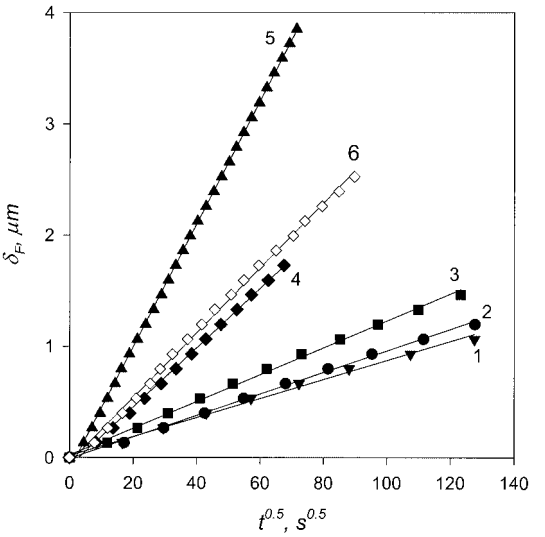

Figure 6 Dependence of δ_F on the square root of t for a treatment with F_2–He mixtures. The compositions of the fluorination mixtures were (1) 2% F_2 and 98% He, (2) 2% F_2 and 98% He, (3) 5% F_2 and 95% He, (4) 10% F_2 and 90% He, and (5) 40% F_2 and 60% He. The total mixture pressure was 1 bar and the treatment temperature was 295 ± 0.5 K for all the compositions. Curve 6 represents the treatment with undiluted fluorine at the same pressure used for curve 4.

The presence of N_2 in a fluorinated mixture slightly affects the rate of formation of a fluorinated layer.

Treatment with the F_2/O_2 mixtures

Usually, the presence of oxygen in a fluorination mixture (so-called oxyfluorination) reduces the rate of

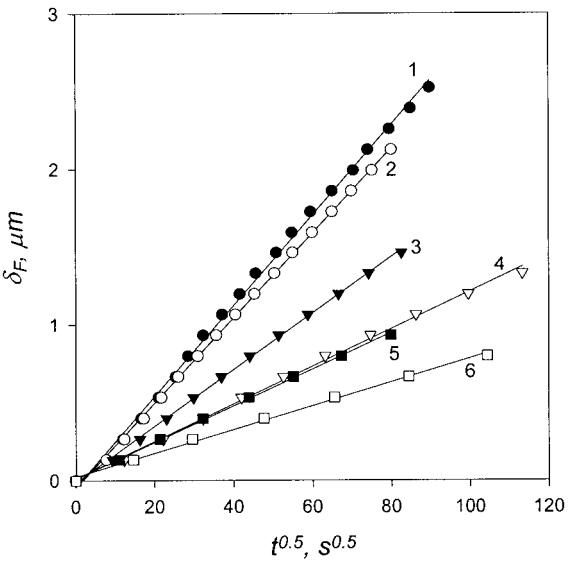

Figure 7 Dependence of δ_F on t for a treatment with F_2–He mixtures. p_F was the same for all the curves, and the p_O/p_F ratios (where p_O is the oxygen partial pressure) were (1) 0, (2) 0.04, (3) 0.12, (4) 0.4, and (5) 1.

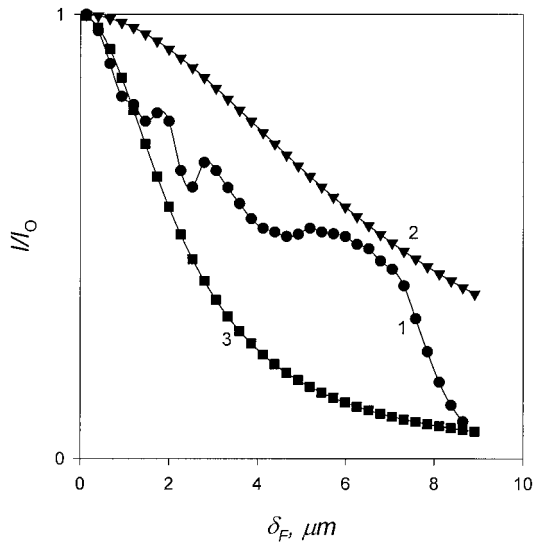

Figure 8 Dependence of the relative intensity (I/I_0) on δ_F: (1) experimentally measured points and (2,3) points calculated with eq. (3) with k values of 0.01 and 0.03, respectively ($\delta_B = k\delta_F$).

formation of a fluorinated layer.[9,12–16] This can be connected to a lower F_2 permeability through the oxyfluorinated layer. The dependence of δ_F on t for F_2/O_2 mixtures of various compositions with fixed p_F values is shown in Figure 7. Oxygen clearly inhibits the fluorination process strongly.

Thus, the rate of formation of a fluorinated layer seems to be limited by F_2 permeation through a fluorinated layer to an untreated one. δ_F depends on t as a square root and practically does not depend on the presence or absence of He and N_2 in a fluorinated mixture, but O_2 strongly inhibits the fluorination process.

The intensity of the interference peaks (I) of the monitored light depends on the thickness of the transition boundary zone (δ_B) as follows:[14,15,23]

$$I/I_0 = [1 + \pi^2(n_V + n_F)^2\lambda^{-2}\delta_B^{-2}]^{-1} = [1 + \pi^2(n_V + n_F)^2\lambda^{-2}k^{-2}\delta_F^{-2}]^{-1} \quad (6)$$

where I_0 is the intensity of the first monitored peak, n_V is the refractive index of the virgin polymer, $\lambda = 0.6328$ μm is the wavelength of the monitored light, and δ_B is equal to $k\delta_F$. The dependence of I/I_0 on δ_F is shown in Figure 8. With consideration given to curves 2 and 3 (Fig. 8), which were calculated on the basis of eq. (6) for $k = 0.01$ and 0.03, the following estimation can be made:

$$\delta_B \leq 0.03\delta_F \quad (7)$$

In addition, fluorination results in a remarkable increase in the PI transparency in the visible and ultraviolet regions (>22,000–50,000 cm^{-1} or ~450–200 nm) of the spectra (Fig. 9).

IR spectra were monitored *in situ* during fluorination: 400 scans were collected for each spectrum (~4 min/spectrum), and 12 spectra were measured in all. All the spectra were corrected for the absorption of ZnSe optical windows. When a film was treated through its entire thickness (fluorination time = 17 h), the fluorine–helium mixture was removed from the reaction vessel, and spectra of the fluorinated film were measured *in vacuo*. Then, atmospheric air was

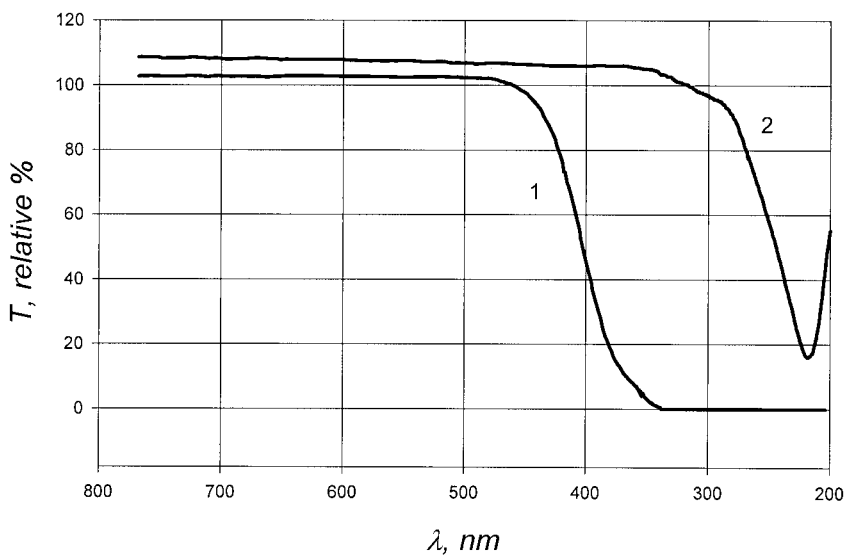

Figure 9 Transmittance (T) of (1) a virgin PI film and (2) a fluorinated PI film cast on a sapphire substrate versus λ. The sapphire substrate, used as a reference spectrum, had a relatively large refractive index ($n \sim 2$); the refractive index of the PI films was close to $n^{0.5}$. The polymer layer acted as an antireflection coating and resulted in T values exceeding 100%.

TABLE I
Assignment of the Absorption Bands of Matrimid® 5218

Wave number (cm^{-1})	Assignment
722 and 711	δ out-of-plane NCO + NCC (1)
826	δ out-of-plane $(CH_3)_2$—C (5) + δ CCH (4)
858	δ out-of-plane CCH (4)
1094	δ in-plane CCH (2,4)
1162	δ in-plane CCH (2,4)
1209	δ in-plane CCC + CCH (5)
1250	ν N—C (1) + δ in-plane NCO (1)
1298	ν N—C (1) + δ in-plane NCO (1)
1374	δ in-plane (CH_3) (5) + δ in-plane NCO (1)
1425	δ out-of-plane NCO + NCC (1)
1488	ν C—C (2,4)
1512	ν C—C (2,4)
1617	ν C—C (2,4)
1673	ν C═O (3)
1725	ν_{sym} C═O (1)
1779	ν_{asym} C═O (1)
2869	ν C—H (5)
2932	ν C—H (5)
2958	ν C—H (5)
3050	ν C—H (2,4)

inserted into the reaction vessel, and this was followed by IR spectroscopy measurements again. The assignment of the IR bands is shown in Table I. The figures in parentheses in column 2 of Table I indicate the location of each group in the PI molecule shown in Figure 1. Many of the absorption bands have a mixed nature. Selected spectra are shown in Figure 10. A reduction of the intensities of CH, CH_2, C═C, and C—N groups is accompanied by an increase in the absorption of CF_n (n = 1, 2, or 3) groups from approximately 900 to 1400 cm^{-1}. Computer simulation was used to separate overlapping peaks and to measure the peak areas. Changes in the total amounts of the following groups were monitored: C═C (1512 and 1488 cm^{-1}), C—H in six-member rings (2,4; 858 cm^{-1}), C—H in five-member rings (5; 2865 and 1209 cm^{-1}), CH_2 in five-member rings (5; 1425 cm^{-1}), C—N (711 and 722 doublet), C═O (3; 1673 cm^{-1}), C═O (1; symmetric 1725 and asymmetric 1779 cm^{-1}), and C(O)F band (1859 cm^{-1}). The band assignment was made on the basis of ref. 25. The accuracy of the peak area calculation was estimated to be ±10%.

Unfortunately, the bands at 3061, 3027, 2960, and 2929 cm^{-1} cannot be used for quantitative calculations because of their low intensity and a significant overlapping with very wide diffuse bands of associated HF. Also, the band at 1425 cm^{-1} becomes very weak when t is greater than 4 min (see Fig. 11) and can be used for qualitative estimations only. Figure 11 indicates that all the CH, C═C, and CN bands disappear more or less simultaneously. This means that hydrogen atoms are replaced with fluorine, double bonds are saturated with fluorine, and at least one C—N bond in the five-member ring is disrupted.

During fluorination, the intensities of all the C═O groups change, and a new absorption band (identified as acid fluoride COF[1,13–21,26]) at approximately 1860 cm^{-1} arises (Fig. 12). The total number of C═O groups practically does not change (curve 1 in Fig. 13) during fluorination. The intensities of ν_{sym} C═O (1) and ν_{asym} C═O (1) are redistributed because of the attachment of a fluorine atom to a carbon atom closest to the C═O group:

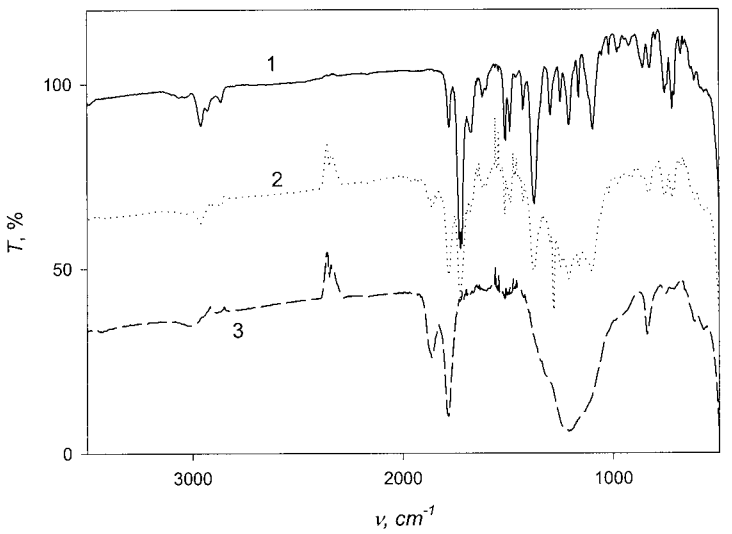

Figure 10 IR spectra of (1) a virgin PI film, (2) a PI film treated with a fluorine–helium mixture (F_2/He = 1:4, total pressure = 1 bar, time = 21 min), and (3) a PI film treated through its entire thickness. The band over 2300–2400 cm^{-1} corresponds to uncompensated CO_2. T is the transmittance.

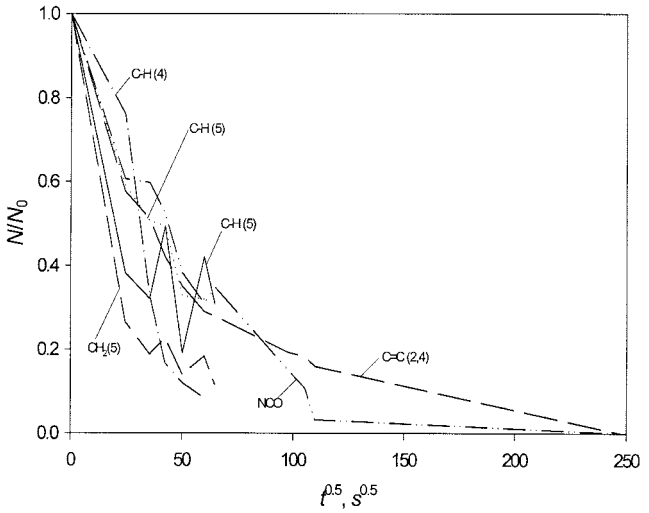

Figure 11 Dependence of the relative number of appropriate groups (N/N_0, where N_0 is the starting number and N is the current number) on the square root of t (F_2/He = 1:4, total pressure = 1 bar, temperature = 295 ± 1 K). The group assignments are shown in the graph.

$$\text{—N—(C═O)—}C_6H_3\text{—} + F_2 \Rightarrow \text{—N—(C═O)—}FC_6H_2\text{—} + HF \quad (8)$$

The addition of fluorine to a carbon atom adjacent to the C═O bond should result in a shift of the absorption band to a higher frequency, from 1725 to 1779 cm^{-1}.

The origin of the 1860-cm^{-1} band can be explained by the disruption of the C—N bond followed by the addition of the fluorine atom to the carbon atom and the formation of the acid fluorine group:

$$\text{—N—(C═O)—}C_6H_3\text{—} \Rightarrow \text{—F—(C═O)—}C_6H_3\text{—} \quad (9)$$

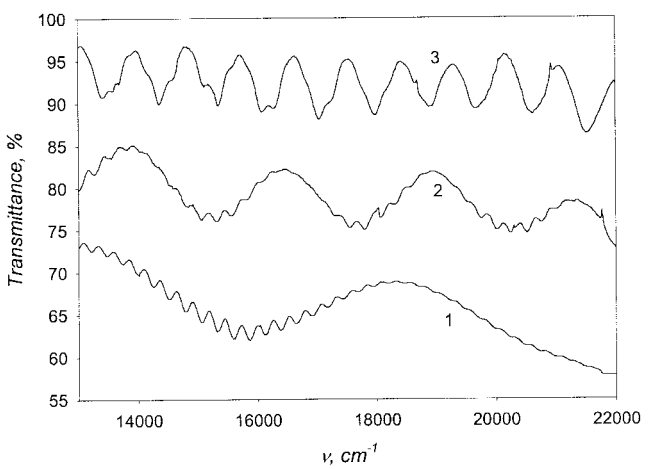

Figure 12 Visible spectra of a free PI film treated step by step with a constant fluorine pressure. t was increased in the sequence 1–2–3.

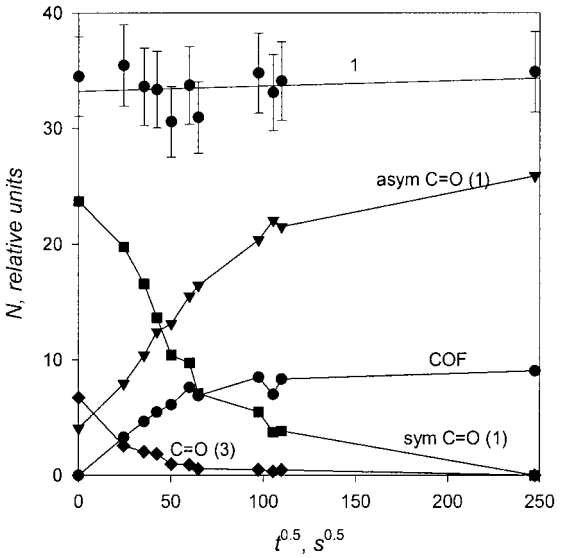

Figure 13 Dependence of the number (N; relative units) of various C═O groups (the assignment is shown in the graph) and the total number of all the C═O groups (top curve 1 summarizes the number of all the C═O groups with error bars) on the square root of t (F_2/He = 1:4, total pressure = 1 bar, temperature = 295 ± 1 K).

The acid fluorine group COF absorbs at 1860 cm^{-1}.

Under evacuation, the total number of C═O groups is reduced by approximately 15% with respect to the number of C═O groups in a virgin polymer measured in the presence of a fluorinated mixture in a reaction vessel. It can be associated with the diffusion of low-molecular-weight fragments outside the film bulk under evacuation. Therefore, a rough estimation can be made: about 15% of the C═O containing groups are dissociated into low-molecular-weight fragments.

To estimate the number of monitored groups in the fluorinated layer (N_F), we applied the following procedure. The total number of CH(4), CH(5), C═C, and CNO groups (N) was calculated with the GRAMS/386 software as described previously. Then, the number of the aforementioned groups in the unmodified layer (N_V) was estimated on the basis of the obtained data as follows:

$$N_V = N_0(\delta_V/11.4) \quad (8)$$

where δ_V is the thickness of the unmodified layer and N_0 · corresponds to the moment when fluorination was not started. It is evident that for all the groups of CH, C═C, and CNO, the following equation is valid:

$$N_F = N - N_V \quad (9)$$

An estimation based on the obtained experimental data and a respective regression analysis of spectral peak areas can provide the following conclusion: the

amounts of CH, CH_3, nondisrupted five-member rings, and C═C bonds inside the fluorinated layer do not exceed by more than approximately 5% their amounts in the starting sample.

The density of polymers is greatly increased under fluorination and usually varies over the approximate range of 1.6–2 g cm^{-3}.[5,10,16–18] It is difficult to measure the density directly, and so the following procedure was applied. PI films were cast onto a solid sapphire support and then removed from it. A flat, parallel free film was selected. That film was treated with fluorine from both sides. The transmission spectrum of the film exhibited interference features in the visible and near-UV regions, as shown in Figure 12. From these data, δ_V and δ_F were measured. A fluorinated film treated from both sides presents a three-layer structure and consists of two layers of fluorinated polymer (F1 and F2) and one layer of unmodified (virgin) polymer (V). Interference phenomenon arise from the interference of the following light beams: (1) a light beam passing through the film without reflection and twice reflected from the F1-air and F2-air surfaces (layer V + F1 + F2); (2) a light beam passing through the film without reflection, twice reflected from surfaces F1-air and F1-V, and twice reflected from surfaces F2-air and F1-V (layer V + F2); (3) a light beam passing through a film without reflection and twice reflected from surfaces F1-air and F2-V (layer V + F1); and (4) a light beam passing through the film without reflection and twice reflected from surfaces F2-V and F1-V (layer V). As we subsequently found, the δ_F values for F1 and F2 are the same, and so we designate a fluorinated layer as F and operate only with layers F, V + F, V + 2F, and V. In this case, the dependence of the intensity of the light (I) passing through a fluorinated film on the wave number, or frequency (ν), can be described by the following expression:

$$I = K\{1 + \alpha_1 \sin[2\pi\nu(n_V\delta_V + 2n_F\delta_F)] + \alpha_2 \sin[2\pi\nu n_F\delta_F] + \alpha_3 sin[2\pi\nu(n_V\delta_V + n_F\delta_F)] + \alpha_4 \sin(2\pi\nu n_V\delta_V)\} \quad (10)$$

where K, a_1, a_2, a_3, and a_4 are constants. Experimental measurements indicated a uniformity of the refractive indices of fluorinated and virgin polymers over the 13,000–18,000 cm^{-1} range: $n_F = 1.41$ and $n_V = 1.63$ with an accuracy ± 0.02.

To measure the thickness of layers F1, F2, and V simultaneously, we applied a fast Fourier transformation to the transmission spectra of the treated films. The aforementioned kinetic interference method[9,13–17] was applied to monitor δ_F. Simultaneously with the measurement of δ_V and δ_F, each sample was weighed after each fluorination stage. The relationship of δ_V and $2\delta_F$ (for a film fluorinated from both sides simultaneously) is shown in Figure 14. A Matrimid® 5218 film expands under fluorine action; that is, the thickness of a completely fluorinated film is greater than the thickness of the initial film. The sample area does not change over the course of treatment. The total mass (m_t) of the film depends on δ_V and δ_F as follows:

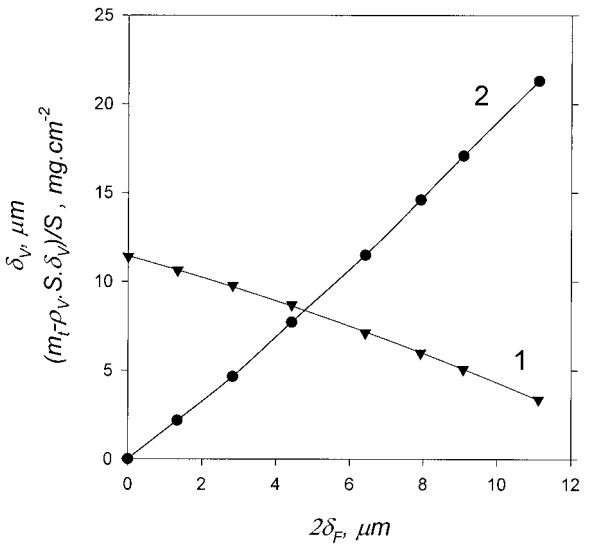

Figure 14 (1) δ_V and (2) $(m_t - \rho_V S\delta_V)/S$ (where ρ_V is 1.24 g cm^{-3} and S is 17.58 cm^2) versus $2\delta_F$.

$$m_t = \rho_V S\delta_V + \rho_F S2\delta_F \quad (11)$$

where $\rho_V = 1.24$ g cm^{-3} is the density of the virgin PI,[21] $S = 17.58$ cm^2 is the film area, and ρ_F is the average density of the fluorinated layer. The dependence of the mass of the fluorinated part of the film $[(m_t - \rho_V S\delta_V)/S]$ on δ_F is shown in Figure 14. Calculated on the basis of these data, the dependence of ρ_F on δ_F is shown in Figure 15. The chemical transformation of Matrimid® 5218 seems to proceed via two stages. During the first stage, the majority of chemical conversion takes place inside the boundary reaction zone [see eq. (7): $\delta_B \leq 0.03\delta_F$) and is accompanied by a refractive-index decrease and a polymer density increase from 1.24 to approximately 1.6–1.7 g cm^{-3}. A further increase in the polymer density to approximately 1.9 g cm^{-3} during the next stage probably proceeds because of (1) postreactions with fluorine resulting in chemical composition changes and (2) the formation of crosslinks via the termination of two adjacent radicals without a change in the chemical composition.

Free (unsupported) Matrimid® 5218 films were used to study the influence of fluorination conditions on the surface energy of PI. Formamide and distilled water were used to measure the total surface energy (γ) and its polar (γ_P) and dispersion (γ_D) components by the method described in refs. 24 and 25. The influence of the treatment conditions on γ, γ_P, and γ_D for PI is shown in Figure 16. It is evident that the surface

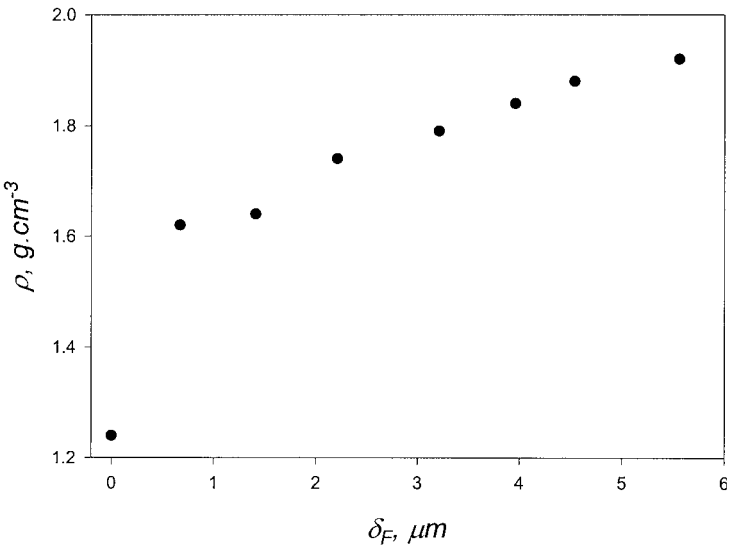

Figure 15 Dependence of ρ_F on δ_F.

energy is markedly changed under fluorine action. An increase in t results in a significant increase in γ followed by a slight decrease (Fig. 16). γ_P and γ_D exhibit more complex behavior. It is evident that γ_P and γ_D can be varied over a wide range by changes in the treatment conditions (e.g., the degree of polarity); that is, the γ_P/γ ratio can be varied from 0.12 to 0.68.

To study the processes of the formation and termination of radicals inside a fluorinated layer, we treated free PI films with a fluorinated mixture of 10% F_2 and 90% He (total mixture pressure = 1 bar, treatment temperature = 21°C). Then, the samples were evacuated, inserted into glass vials, closed, and kept at the temperature of liquid nitrogen (77 K) before the ESR measurements. The time interval between the end of fluorination and this placement was 6 min. The ESR spectra were measured at 77 K. After each measurement, a vial containing a polymer sample was quickly heated to room temperature (20°C) and stored at the same temperature for some time. Then, ESR spectra were measured again, and this process continued. Both peroxy RO_2 (initially, 21–36% with respect to the

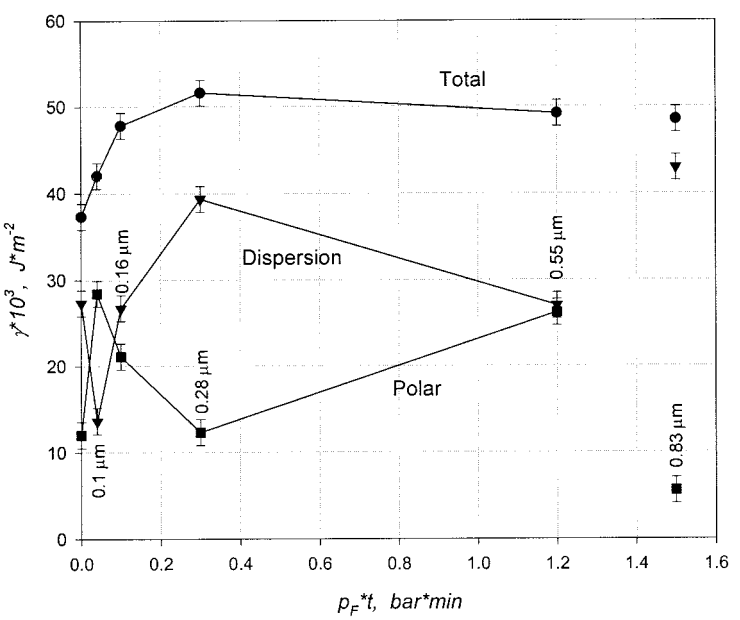

Figure 16 Dependence of (●) γ, (■) γ_P, and (▼) γ_D on the product of p_F and t. For the points connected by lines, 2% F_2/98% He mixtures were used, and t was 0, 2, 5, 15, or 60 min; for the extreme right points, undiluted fluorine was used, and p_F was 1 bar. The treatment temperature was 21°C. The figures in the plot indicate δ_F.

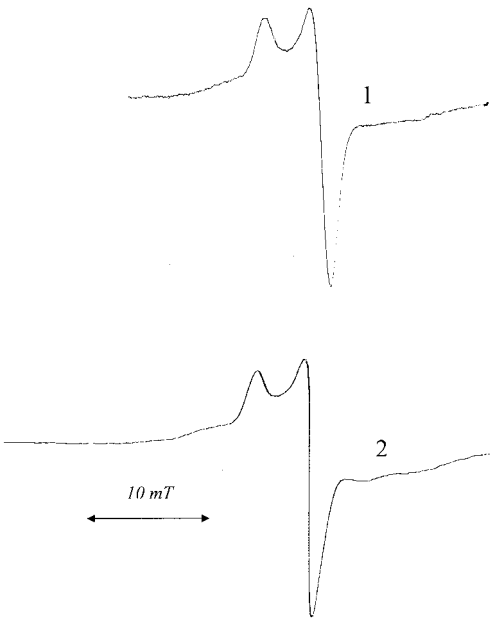

Figure 17 ESR spectra of fluorinated PI films: (1) PIESR02 just after the end of fluorination and (2) PIESR03 stored for 28 h after the end of fluorination at room temperature (294 K).

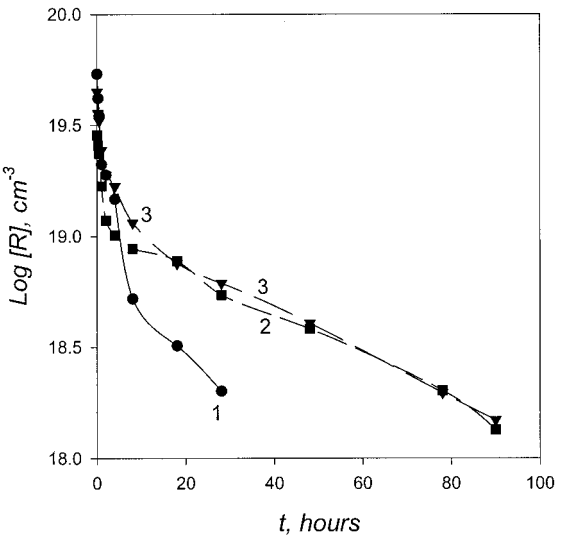

Figure 18 Semilogarithmic dependence of [R] (radicals per cubic centimeter of the fluorinated layer) on t for samples PIESR01, PIESR02, and PIESR03 at room temperature (293 K). For the treatment, a 10% F_2/90% He fluorinated mixture was used, with a total pressure of 1 bar and a temperature of 294 K. t was (1) 5, (2) 18, or (3) 62 min.

total number of radicals) and fluoroalkyl radicals were detected in each experiment (Fig. 17). Fluoroalkyl radicals were evidenced by the wide wings of the ESR spectra and a superfine splitting (ΔH) value characteristic of fluorine-containing radicals: $\Delta H \sim 5.4$–$5.8\ mT$. The experimental conditions are summarized in Table II.

The dependence of the concentration of radicals ([R]; radicals cm^{-3}) on time t (h) at room temperature is shown in Figure 18. The concentration of radicals in fluorinated PI is reduced by a factor of 2 in approximately 1 h. However, the termination rate then strongly decreases. There are two distinct regions of radical termination kinetics: 0–2 h and greater than 2 h. The termination of both peroxy and fluoroalkyl radicals in samples PIESR01 and PIESR02 proceeds practically synchronically. However, for sample PIESR03, peroxy radicals terminate more quickly than fluoroalkyl radicals (see the last column in Table II).

A half-decay time of peroxy radicals in fluorinated Matrimid® 5218 is close to several hours. This time is sufficient to carry out the graft polymerization of the respective monomers. The graft polymerization of acrylonitrile (AN) to freshly fluorinated Matrimid® 5218 films cast on ZnSe supports was carried out. IR spectroscopy was used to measure the amount of the grafted polymer. To detect and evaluate the amount of grafted polyacrylonitrile (PAN), we cast a film of PAN from a solution in dimethylformamide (DMFA), and the IR spectrum of that film was measured. The most marked feature of the PAN spectrum was a strong —C≡N band at approximately 2244–2245 cm^{-1}, so

TABLE II
Monitoring of Radical Creation in Fluorinated PI

	Sample		
	PIESR01	PIESR02	PIESR03
Fluorination mixture	10% F_2 + 90% He	10% F_2 + 90% He	10% F_2 + 90% He
Total mixture pressure (bar)	1	1	1
Treatment duration (min)	5	18	62
Treatment temperature (°C)	20.7	20.7	20.7
Thickness of fluorinated layer from one side (μm)	0.38	0.8	1.55
Maximum concentration of radicals/cm^3 of fluorinated layer	5.4×10^{19}	4.5×10^{19}	2.9×10^{19}
Amount of peroxy radicals with respect to the total amount of radicals (%) just after the end of fluorination	~21	~26	~36
Amount of peroxy radicals with respect to the total amount of radicals (%) in 28 h after the end of fluorination	~21	~26	~18

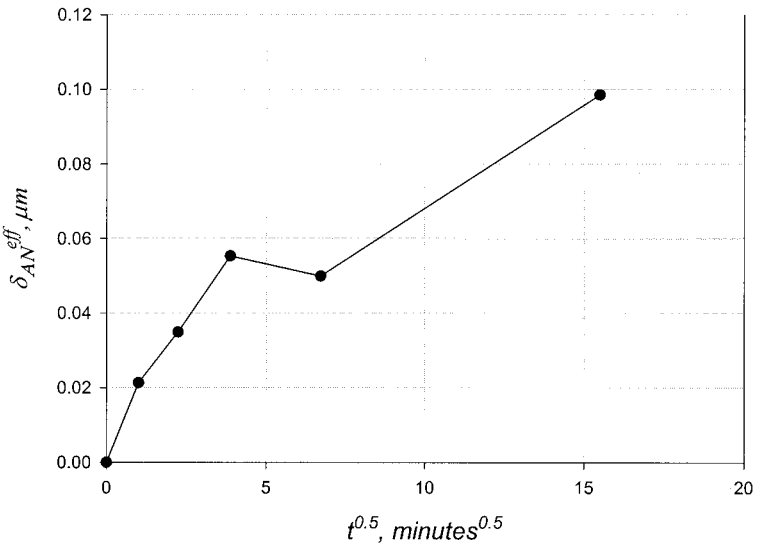

Figure 19 Dependence of δ_{AN}^{eff} on the square root of t.

that band was used to identify and measure the amount of grafted PAN. The area (W) of that band in the absorption mode (i.e., log T, where T is the transmittance) for a cast PAN film was equal to $W = 2.5$ cm^{-1}, and the thickness of the film (δ) was equal to $\delta = 3.13$ μm, so the extinction coefficient (ϵ) for the aforementioned band ($W = \epsilon\delta$) could be estimated to be $\epsilon = 0.80$ cm^{-1} μm^{-1}. This ϵ value was used to calculate the effective thickness of grafted AN (δ_{AN}^{eff}) as follows:

$$\delta_{AN}^{eff} = W\varepsilon^{-1} \tag{12}$$

All the samples were treated with undiluted fluorine at a total pressure of $p_F = 0.1$ bar for 20 min. δ_F was 0.97 μm. Then, the reaction vessel with the polymer sample was evacuated and filled with AN at 0.07 bar. t was varied from 0 to 4 h. The dependence of δ_{AN}^{eff} on the square root of t is shown in Figure 19. The maximum δ_{AN}^{eff} value was close to 0.073 μm and reached approximately 7.5% with respect to δ_F.

CONCLUSIONS

The fluorination of PI films with undiluted fluorine and fluorine–helium, fluorine–nitrogen, and fluorine–oxygen mixtures is a diffusion-controlled process. This means that the rate of formation of a fluorinated layer is limited by the rate of permeation of fluorine through the fluorinated layer to the boundary transition zone. A fluorine-treated film consists of layers of mainly fluorinated and virgin (untreated) polymers that are separated by a very thin boundary transition layer, in which the main chemical transformations proceed. The dependence of δ_F on t and the fluorine, helium, nitrogen, and oxygen partial pressures has been studied quantitatively. For all the fluorinated mixtures, δ_F is approximately equal to $t^{0.5}$; oxygen inhibits the rate of formation of a fluorinated layer, but helium and nitrogen practically do not influence the rate of reaction. The thickness of the boundary (transient) zone has been estimated to be $\delta_B \leq 0.03\delta_F$. With IR and UV spectroscopy, we have shown that during fluorination, hydrogen atoms are replaced by fluorine, double bonds are saturated with fluorine, and at least one C—N bond in the five-member ring is disrupted. Fluorination results in a significant increase in the polymer density and a decrease in the refractive index. The fluorination of PI films results in an increase in their transparency in the visible and ultraviolet regions of spectra. Additionally, γ_P and γ_D can be varied over a wide range through changes in the treatment conditions (e.g., the degree of polarity); that is, the γ_P/γ ratio can be varied from 0.12 to 0.68. The direct fluorination of PI Matrimid® 5218 generates a relatively high concentration (up to $\sim 5 \times 10^{19}$ radicals/cm^3 of fluorinated layer) of long-living radicals inside the fluorinated polymer layer. There are two distinct regions of radical termination kinetics: 0–2 h and greater than 2 h. The kinetics of formation of a PAN layer via the postgrafting of AN have been studied. The maximum δ_{AN}^{eff} value is close to 0.073 μm and reaches approximately 7.5% with respect to δ_F. The data obtained in this study can be used in the controlled modification of any articles made from PI Matrimid® 5218, including membranes.

The authors are grateful to G. N. Bondarenko (A. V. Topchiev Institute of Petrochemical Synthesis, Moscow, Russia) for the interpretation of the IR spectra and to G. H. Koops (Twente University, Enschede, The Netherlands) for the polymer samples and a fruitful discussion.

References

1. Lagow, R. J.; Margrave, J. L. Prog Inorg Chem 1979, 26, 162.
2. Jagur-Grodzinski, J. Prog Polym Sci 1992, 17, 361.
3. Anand, M.; Hobbs, J. P.; Brass, I. J. In Organofluorine Chemistry: Principles and Commercial Applications; Banks, R. E.; Smart, B. E.; Tatlow, J. C., Eds.; Plenum: New York, 1994; p 469.
4. Johns, K. Proceedings of the 4th International Conference on Fluorine in Coatings, Brussels, Belgium, March 2001; Paper 1.
5. Kharitonov, A. P. J Fluorine Chem 2000, 103, 123.
6. Busygin, V. B.; Syrtsova, D. A.; Teplyakov, V. V. Proceedings of Euromembrane 99, Leuven, Belgium, Sept 1999; Vol. 2, p 516.
7. Borisov, S. B.; Khotimsky, V. S.; Slovetsky, D. I. J Membr Sci 1997, 125, 319.
8. Kolpakov, G. A.; Kuzina, S. I.; Kharitonov, A. P.; Moskvin, Yu. L.; Mikhailov, A. I. Sov J Chem Phys 1992, 9, 2283.
9. Kuzina, S. I.; Kharitonov, A. P.; Moskvin, Yu. L.; Mikhailov, A. I. Russ Chem Bull 1996, 45, 1623.
10. Kharitonov, A. P. Popular Plast Packaging 1997, 42, 75.
11. Kharitonov, A. P.; Moskvin, Yu. L.; Kolpakov, G. A. Rus. Pat. N 1,754,191 (1990).
12. Frolov, V.; Teplyakov, V. V.; Kharitonov, A. P. Conference Papers of the 2nd International Conference on Fluorine in Coatings, Salford, England, Sept 1994; Paper N 22.
13. Kharitonov, A. P.; Moskvin, Yu. L.; Kharitonova, L. N.; Tulskii, M. N.; Kotenko, A. A. Mendeleev Commun 1994, 3, 91.
14. Kharitonov, A. P.; Moskvin, Yu. L.; Kharitonova, L. N.; Kotenko, A. A.; Tulskii, M. N. Kinet Catal 1994, 35, 792.
15. Kharitonov, A. P.; Moskvin, Yu. L.; Kharitonova, L. N.; Kotenko, A. A.; Tulskii, M. N. Polym Sci Ser B 1995, 37, 307.
16. Kharitonov, A. P.; Moskvin, Yu. L. J Fluorine Chem 1998, 91, 87.
17. Kharitonov, A. P.; Moskvin, Yu. L.; Teplyakov, V. V.; Le Roux, J. D. J Fluorine Chem 1999, 93, 129.
18. Kharitonov, A. P.; Taege, R.; Ferrier, G.; Piven, N. Conference Papers of the 5th International Conference on Fluorine in Coatings, Orlando, FL, Jan 2003; Paper 7.
19. Pud, A. A.; Rogalsky, S. P.; Shapoval, G. S.; Kharitonov, A. P.; Kemperman, A. Polym Degrad Stab 2000, 70, 409.
20. Pud, A. A.; Rogalsky, S. P.; Shapoval, G. S.; Kharitonov, A. P.; Teplyakov, V. V.; Strathmann, H.; Poncin-Epailard, F. Polymer 2001, 42, 1907.
21. Taege, R.; Ferrier, G.; Kharitonov, A. P. Proceedings of the 16th European Symposium on Fluorine Chemistry, Durham, England, July 2000; A34.
22. Bos, A. Ph.D. Thesis, Twente University, 1996.
23. Kharitonov, A. P.; Moskvin, Yu. L.; Kolpakov, G. A. Polym Sci USSR 1985, 27, 739.
24. Owens, D. K.; Wendt, R. C. J Appl Polym Sci 1969, 13, 1740.
25. Van Krevelen, D. W. Properties of Polymers: Correlations with Chemical Structure; Elsevier: Amsterdam, 1972.
26. Socrates, G. Infrared Characteristic Group Frequencies, 2nd ed.; Wiley: Chichester, England, 1994.